








Article

Quantitative Evaluation of the Emissions of a Transport Engine Operating with Diesel-Biodiesel

Armando Pérez ^{1,*}, David Mateos ², Conrado García ², Camilo Caraveo ¹,
Gisela Montero ², Marcos Coronado ² and Benjamín Valdez ²

¹ Facultad de Ciencias de la Ingeniería y Tecnología, Universidad Autónoma de Baja California, Blvd. Universitario #1000, Unidad Valle de las Palmas, Baja California CP. 21500, Mexico; camilo.caraveo@uabc.edu.mx

² Instituto de Ingeniería, Universidad Autónoma de Baja California, Blvd. Benito Juárez y Calle de la Normal S/N, Col. Insurgentes Este, Mexicali, Baja California 21280, Mexico; david.mateos@uabc.edu.mx (D.M.); cnrdgarcia@uabc.edu.mx (C.G.); gmontero@uabc.edu.mx (G.M.); coronado.marcos@uabc.edu.mx (M.C.); berval@uabc.edu.mx (B.V.)

* Correspondence: armando.perez.sanchez@uabc.edu.mx

Received: 22 May 2020; Accepted: 2 July 2020; Published: 13 July 2020



Abstract: The present work is about evaluating the emission characteristics of biodiesel-diesel blends in a reciprocating engine. The biodiesel was produced and characterized before the test. A virtual instrument was developed to evaluate the velocity, fuel consumption, temperature, and emissions of O₂, CO, SO₂, and NO from an ignition-compression engine of four cylinders with a constant rate of 850 rpm. The percentages of soybean-biodiesel (B) blended with Mexican-diesel (D) analyzed were 2% B-98% D (B2), 5% B-95% B (B5), and 20% B-80% D (B20). The biodiesel was obtained through a transesterification process and was characterized using Fourier-Transform Infrared spectroscopy and Raman spectroscopy. Our results indicate that CO emission is 6%, 10%, and 18% lower for B2, B5, and B20, respectively, in comparison with 100% (D100). The O₂ emission is 12% greater in B20 than D100. A reduction of 3% NO and 2.6% SO₂ was found in comparison to D100. The obtained results show 44.9 kJ/g of diesel's lower heating value, this result which is 13% less than the biodiesel value, 2.8% less than B20, 1.3% than B5, and practically the same as B2. The specific viscosity stands out with 0.024 Poise for the B100 at 73 °C, which is 63% greater than D100. The infrared spectra show characteristics signals of esters groups (C-O) and the pronounced peak from the carbonyl group (C=O). It is observed that the increase in absorbance of the carbonyl group corresponds to an increase in biodiesel concentration.

Keywords: virtual instrument; LabVIEW; characterization; diesel-biodiesel; emissions; infrared spectra

1. Introduction

In recent decades, many studies on biofuels have been conducted to reduce air pollution generated primarily by internal combustion engines (ICEs). The ICE is used in different means of transport as well as in other internal combustion equipment. As above, the dependence on fossil fuels has increased without neglecting the decrease in the production of petroleum-based energetics [1–3]. It is important to take into account that the increase in fossil fuels consumption also produces an increase in environmental problems. Considering the Statistical Review of World Energy issued by the British Petroleum Statistical Review (BP), it was mentioned that in 2016, the global consumption of primary energy increased 1% with respect to the 0.9% of 2015, and in turn, the production and consumption of all the fuels increased except the production of nuclear energy [4]. The worldwide production of biodiesel was 25 billion L in 2013, and in 2015 it increased to 129 billion L approximately. It represents an increment of 5.1% [5,6].

There are many studies concerning the use of biodiesel as a substitute for diesel, but this proposal was not recent. From the invention of the compression ignition engine (CIE), Rudolf Diesel proposed the use of 100% peanut oil as fuel for the engine operation. Later, many subsequent studies have shown that vegetable oils used to produce biodiesel can be renewable. The studies reveal that it is easy to produce and has a high calorific value. Other research works have been developed to improve biodiesel characteristics like the poor flow and low volatility at low temperatures [7–9].

Biodiesel is considered an alternative biofuel to diesel, because it can be produced with oils that come from vegetables or animal fat, making it biodegradable and renewable. The CIE's emissions coming from the combustion contains up to 10% oxygen in its structure, this promotes better combustion because it turns oxygen into a more oxygenated fuel that favors a complete and efficient combustibles, reducing the non-burned hydrocarbon production and suspended particles. The environmental impact in CO₂ terms is strongly affected by the absorption of this gas by plants during its growth [10–13]. Another main biodiesel advantage is that it does not contain carcinogens as polychromatic and polyaromatic nitrided hydrocarbons (PNHs), producing less harmful health contamination when it is burned inside the combustion chamber [14–16].

There are different tools to measure the CIE's emissions, some equipment is portable or stationary. This equipment normally has a high price and does not have the option to modify the measurement range, which makes them a rigid tool, and they are limited to specific applications without having the versatility and flexibility to adapt them to other required uses [17,18]. Virtual instrumentation (VI) establishes a technology based on the use of software systems, hardware, and a computer. It replaces a measurement and control system in the real world, any program and hardware that fulfills this function [19,20]. In almost all commercial systems, the concept of VI is realized in an object-oriented programming language, modern scientific instrumentation, development, and evolution of VI-based systems [21,22]. The main advantages are (i) versatility and performance of the software and hardware; (ii) the reduced cost for acquisition of a sensor channel, in comparison to traditional rigid hardware systems; (iii) combination of the non-exclusive operating hardware with powerful software that results in a scalable architecture instrument, which means the possibility of being modified if necessary [23]. Therefore, the implementation of VI for measuring CIE's emissions is feasible, due to the need to monitor the implementation of biodiesel and verify its impact compared to diesel.

There are many studies, which prove the reduction of emissions by the use of biofuels. It has to be expected that the implementation of the use of biodiesel reduces the CO₂ emissions by using a mixture of diesel-biodiesel as fuel in substitute of diesel [24,25]. However, some research groups report that NO_x emission does not change and sometimes an increase occurs [26–29]. It is reported that the biodiesel has a lower calorific value than diesel, this has a direct repercussion on the power generated by the CIE, derived from a higher consumption to counteract the power demanded by the user [30,31]. Some of the models of vehicles with more recent diesel engines have the characteristic to endure mixtures of diesel-biodiesel until 20% of the second one (B20), offering the advantages of biofuel implementation without affecting the engine efficiency.

The aim of this work is to assess the technical operation of a CIE using the following mixtures: B2 (98% biodiesel–2% diesel), B5 (95% biodiesel–5% diesel), B20 (80% biodiesel–20% diesel), B100 (100% biodiesel), and D100 (100% diesel). The biodiesel was obtained through a transesterification process from soy oil. Raman and Fourier-transform infrared (FTIR) spectroscopy were used to analyze the mixtures. Additionally, physicochemical properties of mixtures, such as calorific value and viscosity were determined.

Another novelty is the development of a virtual instrument using the LabVIEW program for emissions monitoring. Currently, the emissions measurement is performed by gas analyzers based on electrochemical and infrared techniques. Hence, the program, in the form of an interactive graphical user interface, is an additional innovation. The developed VI assesses the specific fuel consumption, temperature from the exhaust gas, engine temperature, and the emission of the exhaust gases: O₂, CO,

SO₂, and NO. The basic parameters of Mercedes-Benz 9004 engine are shown in Table 1, this type of engine is commonly used in urban transportation trucks in Mexicali, Mexico.

Table 1. Parameters of Mercedes-Benz 9004 engine.

Parameter	Value	Unit
Number of cylinders	In-line four cylinders	-
Cylinder diameter	102	mm
Stroke	130	mm
Displacement volume	4.25	lt
Compression ratio	17.4:1	-
Rated power at 2300 rpm	141.7	kW
Maximum torque at 1200–1600 rpm	705.02	Nm
Intake valve	2	-
Exhaust valve	1	-
Decompression valve	1	-
Redline	2300	-
Injection	Direct injection	-

2. Materials and Methods

2.1. Virtual Instrument for Measuring Engine Parameters

The virtual instrument developed to measure engine parameters (VIMEP) is composed of four systems. The first comprises temperature sensors, revolutions per minute, fuel consumption, and O₂, NO, CO, SO₂ gas content. A Faraday cage was used to isolate electromagnetic noise, which could cause interference and alterations in the sensors used for emission readings. The second system consists of conditioners and signal amplifiers for each sensor. In third place, the Data Acquisitions Systems (DAQ) board and the PC with the virtual instrument. Finally, the fourth system is the acquisition and data processing DAQ board 6009 USB model, with eight analogic input of 14 bits, 48 kS/s, and two static analogic output of 12 bits, 12 digital input-output, and a 32-bit counter by National Instruments. The digital signals are transferred to the Lenovo Intel[®] Core[™] i7-471CHQ CPU at 2.50 GHz with Windows 10 operating system. Table 2 shows the properties and operating ranges of each sensor used to detect each type of emission. The sensors have an infrared and electrochemical response [22].

Table 2. Properties and operation range of sensors.

Sensor Properties	Ranges			
	O ₂	CO	SO ₂	NO
Concentration ranges (ppm)	0–30	0–500	0–2000	0–2000
Sensitivity (ppm)	N/A	55–85	8–20	320–480
Maximum overload	100%	1500 ppm	N/A	1000 ppm
Resolution	0.1%	1 ppm	5 ppm	0 to 4.5 ppm
Response time (s)	15–90	30–90	60–90	35–90
Temperature range (°C)	–20 to +55	–20 to +50	–20 to +50	–20 to +50
Relative humidity (%)	15–95	15–90	15–90	15–90
Pressure range (kPa)	90–110	90–110	90–110	90–110

In Figure 1, we can observe the block programming diagram that constitutes the VIMEP used for the characterization of the CIE when works with diesel-biodiesel mixtures.

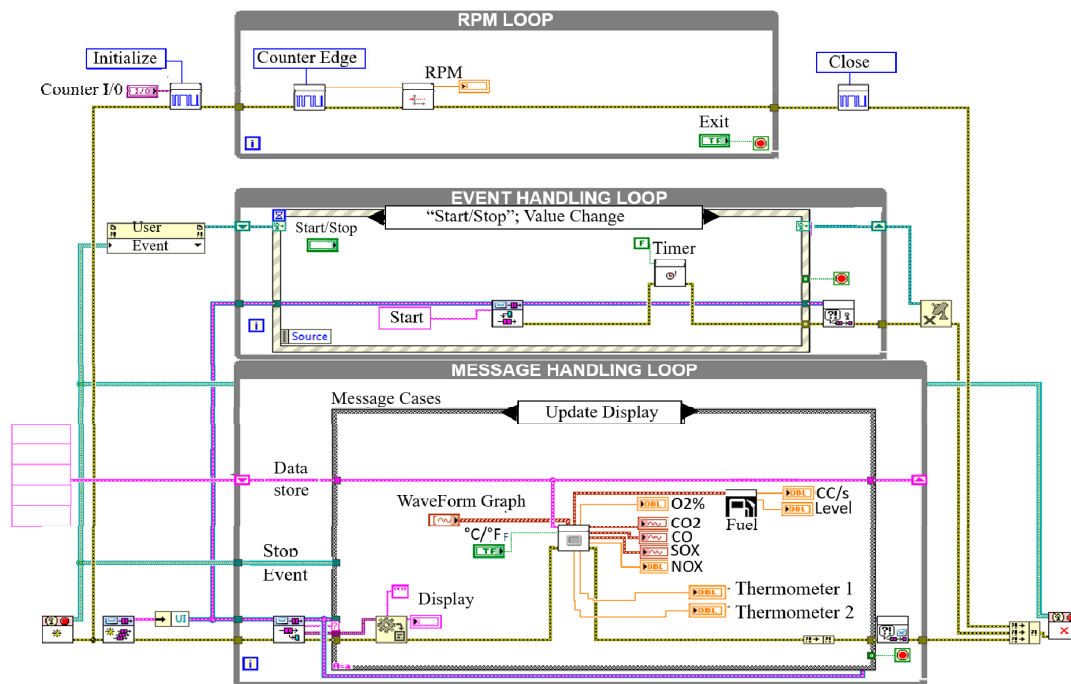


Figure 1. The programming of main blocks of VIMEP.

2.2. Fuel and Its Mixtures Elaboration

Soybean oil was used to obtain biodiesel. Furthermore, to remove the moisture present in the oil, the oil was preheated to 110 °C. The transesterification method was implemented, in which sodium methoxide and soybean oil were treated. The chemical reaction was carried out for 1 h at 60 °C with agitation. A funnel was used to separate the glycerin and biodiesel by density difference, a volumetric ratio of 4:1 was used to wash the biodiesel with water. The final step consisted of heating the biodiesel to 110 °C, to evaporate the biodiesel water from the biodiesel [32–35]. The biodiesel was prepared in the Institute of Engineering of the Autonomous University of Baja California (UABC). The fuel mixtures were characterized using a CAP 2000+ viscometer and to determine the kinematic viscosity of Mexican diesel a value between 1.9 and 4.1 mm²/s was used from PEMEX data sheet [36]. The calorific value was determined using an IKA C2000 calorimeter. For the measurements, approximately 0.5 g were placed inside the equipment and duplicate tests were performed to determine the average value of heat released by combustion of the fuel mixture. Additionally, the optical characterization of the fuels was carried out to obtain their characteristic spectra. For Raman spectroscopy, a Perkin-Elmer Raman Station 400F with a 785 nm laser at room temperature was used. Additionally, FTIR spectra were measured by Perkin Elmer Spectrum One FTIR spectrometer in the range of 400–4000 cm⁻¹ and 4 cm⁻¹ resolutions. The uncertainties of the engine performance and calibration of the measuring instruments, as well as environmental conditions, were then determined for the measured and calculated values. The percentage uncertainties of the measuring instruments used in this study are tabulated in Table 3. Each parameter was measured three times to reduce the uncertainties of the observed values and the average value was then determined. The percentage uncertainty of the engine performance and exhaust emission parameters measured in this study was found to be around 1%, which is deemed satisfactory.

Table 3. Percentage uncertainty of the measuring instruments.

Measured Parameter	Measurement Range	Accuracy	Measurement Sensor	Percentage Uncertainty (%)
Engine speed (rpm)	0–10,000	±1	Magnetic pickup speed transducer	±0.1
Time (s)	-	±0.1	-	±0.2
Fuel flow (mL/min)	20–6000	±10	Flow Sensor Meter	±2
Viscometer (Poise)	0.2–15,000 Poise	<1 mL	Speed of Rotation 5–1000 RPM	±0.5
Calorimeter (J)	0–40,000	±1	Temperature sensor	±0.2
RAMAN spectroscopy	95–3500 cm ⁻¹ Raman shift	4 cm ⁻¹ FWHM Pear resolution and 1 cm ⁻¹ Pixel resolution	High sensitivity open electrode CCD detector, 1024 × 256 pixels sensor hermetically sealed vacuum	
Fourier-Transform Infrared spectroscopy	350–7800 cm ⁻¹	0.5 to 64 cm ⁻¹	785 nm laser at room temperature was used	

2.3. Operation Conditions of CI-Engine

The engine works with B2, B5, and B20 mixtures and D100. Three repetitions were carried out for each mixture under the following conditions: controlled ambient temperature 23 °C with a variation of +/-1 °C, the air supply to the engine of 1 atm of pressure, a relative humidity of 40% with a variation of +/-5%, and 2 L of fuel as initial volume. When a fuel change is made, the fuel tank, lines, fuel filters, priming pump, high-pressure pump are purged and finally, the engine is turned up for 20 min, to ensure that no residue of the previous mixture remains inside the system. The physical measurement system of emissions has a heat exchanger. To guarantee the right function of the sensors the temperature of the gases was set at 50 °C, also three general humidity and four individuality traps were added. The operation of all systems together is explained, starting from the ICE with a copper pipeline reduction from 4 to 1/2 in. of diameter, two safety valves to control the pressure and the exhaust gas flow. The gases continue their way to a heat exchanger where the temperature is reduced from 60 to 35 °C. In a straight way, the gases flow through two gas condensate traps and two humidity traps placed in series, when the gas comes out from the humidity traps it goes to individual humidity traps for each gas. Then the gases are analyzed and finally exhausted into the atmosphere. During the process, the temperature, consumption, and rpm of each test were recorded. Figure 2 shows a diagram that explains the electricity connections, fuel lines, water, air, exhaust gases, communication cables, and equipment used.

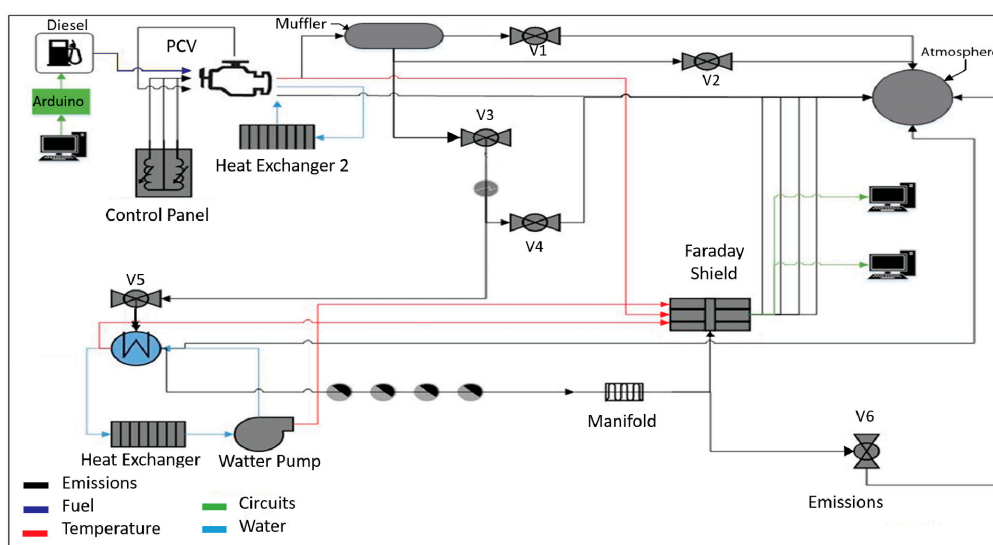


Figure 2. Systems set diagram.

3. Results and Discussions

3.1. Specific Viscosity of the Mixtures

To determine the viscosity of each fuel, three measurements were made for each sample and an average was obtained. Figure 3 shows an average of kinematic viscosity in a temperature range of 50–90 °C for B100, D100, and mixtures B2, B5, and B20 [32,35,36]. The viscosity of the B100 stands out with 0.024 Poise at 73 °C and it is 63% higher than the D100.

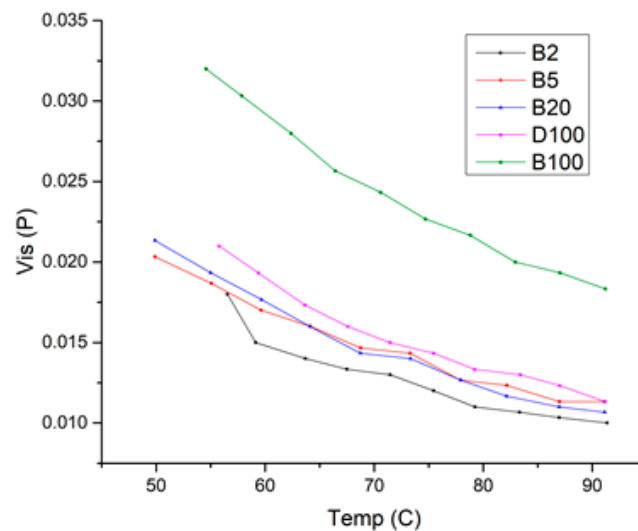


Figure 3. Viscosity vs. temperature.

3.2. Low Calorific Power of Fuels

An overall average of the lower calorific power of 44.97 kJ/g was obtained. Figure 4 shows that the increases in the percentage of biodiesel contained in the mixtures are proportional to the reduction of calorific values. The value for the B100 sample was 39.08 kJ/g and is close to the value of 37.50 kJ/g based on the molecular weight of methyl esters of soybean that are in agreement with those published in the literature [36–38].

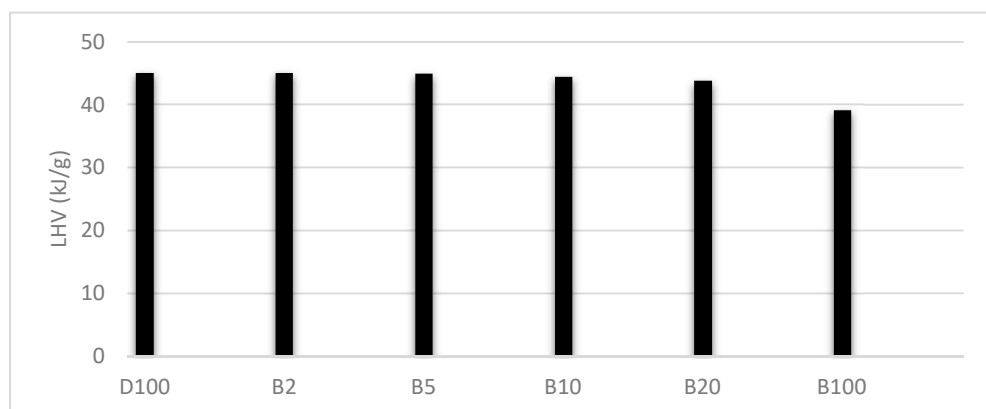


Figure 4. Low calorific values of the fuels.

3.3. Raman Analysis

Raman spectroscopy was carried out to obtain information about organic and inorganic compounds contained in B100, D100, and the different mixtures. Figure 5 shows the characteristic spectrum for D100, B100, B2, B5, and B20, where a bandwidth in $\approx 2800\text{--}3000\text{ cm}^{-1}$ is observed and some characteristic

peaks at 1450, 1306, 1076, and 837 cm^{-1} are also observed. The obtained results indicate that there is no presence of molecules of other substances and our results coincide with those reported in the literature [39,40], which helps us to guarantee the good quality of our biodiesel.

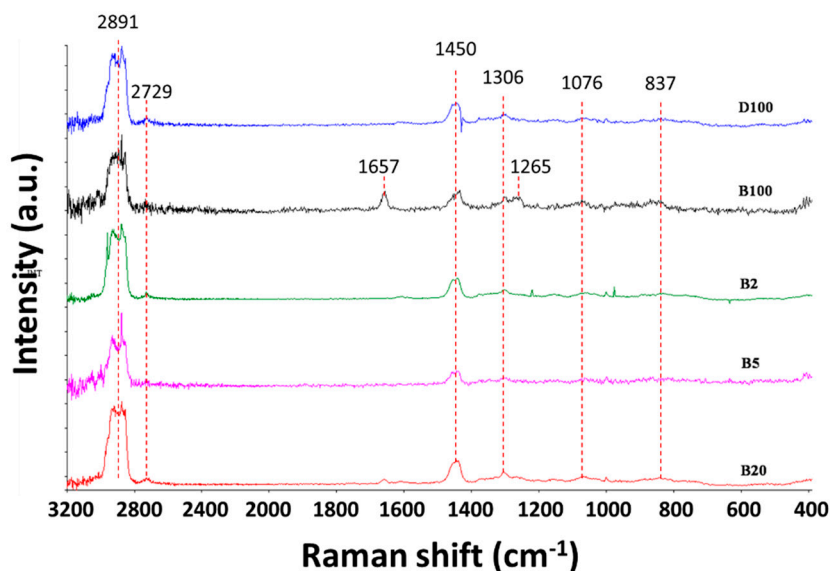


Figure 5. Raman spectra comparison of D100, B100, B2, B5, and B20.

3.4. FTIR Analysis

When comparing the spectra of Figure 6a,b, characteristic biodiesel signals that are absent in the diesel are observed. The IR spectrum of PEMEX diesel exhibits a characteristic double peak at 1457 and 1377 cm^{-1} . Two groups of absorption bands of the methyl esters are shown, and in the region of the fingerprints, the band is between 1200 and 1300 cm^{-1} originating from the asymmetric CO axial deformation. In the region of the functional groups between 1750 and 1730 cm^{-1} , the intense peak corresponds to the carbonyl group (C=O), so the characteristic of the esters is found and related to relatively constant and interference-free stretching vibration [41,42]. This signal being the major difference with the diesel spectrum. For both spectra, the absorption band at 2950–3000 cm^{-1} , corresponds to the stretching of the bonds of aliphatic carbons: CH₃, CH₂, and CH. Additionally, the spectra of soybean-biodiesel mixture are presented at 2% (Figure 6c), 5% (Figure 6d), and 20% (Figure 6e), respectively. A decrease in the intensity of the peaks can be observed as the presence of biodiesel increases

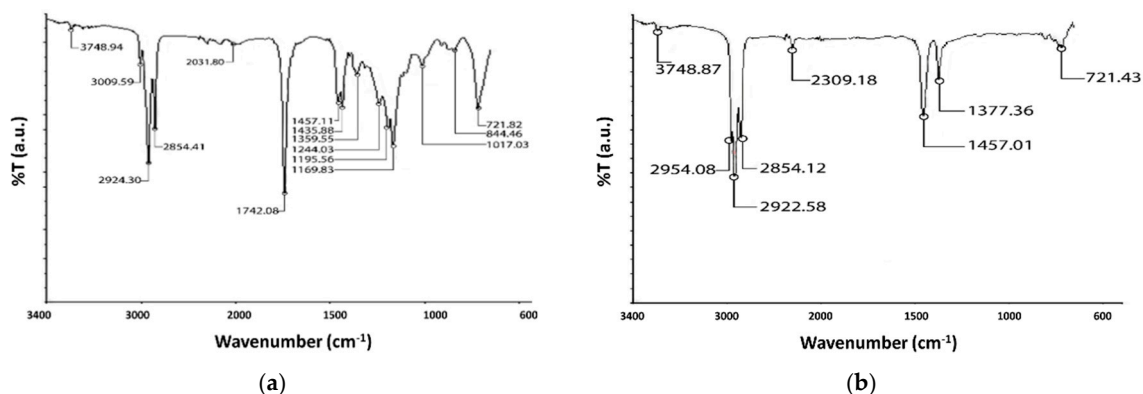


Figure 6. Cont.

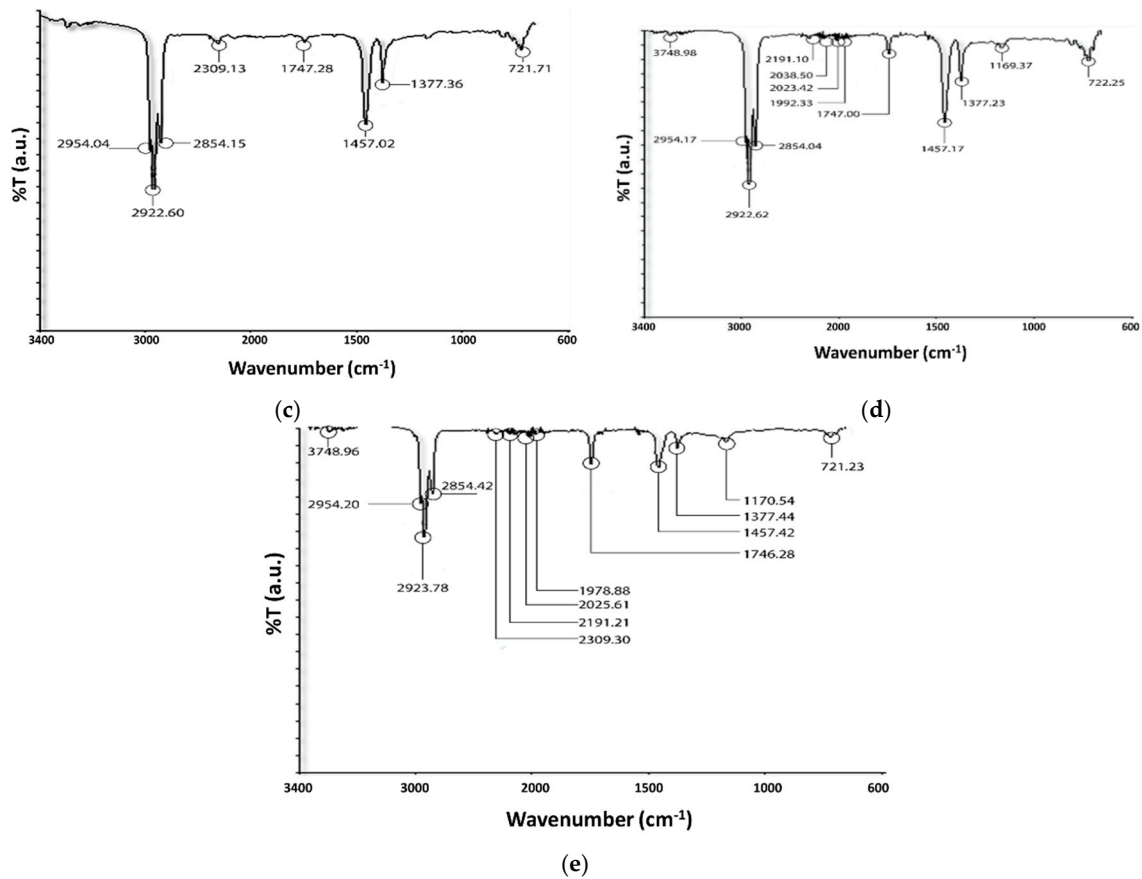


Figure 6. Fourier-transform infrared (FTIR) spectra in transmission mode, characteristic of B100 (a), D100 (b), and the mixtures B2 (c), B5 (d), and B20 (e).

3.5. Results of Fuel Tests

Figure 7 shows the interface of the VIMEP focus in the characterization of CIE using the diesel-biodiesel mixtures. The measuring of the set of parameters is a flexible tool and easily adjustable to the required emission type for a better evaluation of the CIE performance that uses conventional fuels, biofuel, or both. The system presented is not restricted to engines with a specific capacity, it presents the flexibility of being able to adapt to different CIE. For the above, the following aspects must be taken into consideration: operation capacity, fuel consumption, conditions of operation, and used fuel. The VIMEP developed in this investigation is constituted by sensors with a wide range of operation, a plotter that allows you to visualize the saved data of realized tests, thus analyzing, comparing, and importing in real-time the results of the tests.

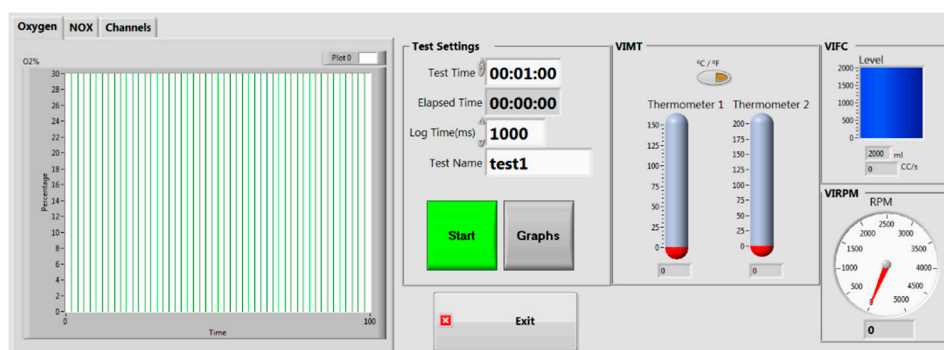


Figure 7. Graph of the interface of the VIMEP for the user.

The result indicates a decrease of calorific value in each mixture: B20 = 2.87%, B5 = 1.33%, and B2 does not present a significant change for diesel, which was the fuel that presents the highest calorific value. The increase of 7.7% in the fuel consumption when working at 850 rpm using the B20 mixture [36–38] was to be expected, because the diesel molecule has a dioxygen molecule and this can be reflected in more efficient combustion inside the combustion chamber of the CI-Engine [43,44]. As a result, an average total fuel consumption was obtained for each mixture of B2 = 1281.92 mL/h, B5 = 1356.58 mL/h, B20 = 1716.37 mL/h, and for the D100 = 1356.58 mL/h is shown in Figure 8. An average of 14% of O₂ emissions was measured for diesel and 12.7% for B20, as can be seen in Figure 9.

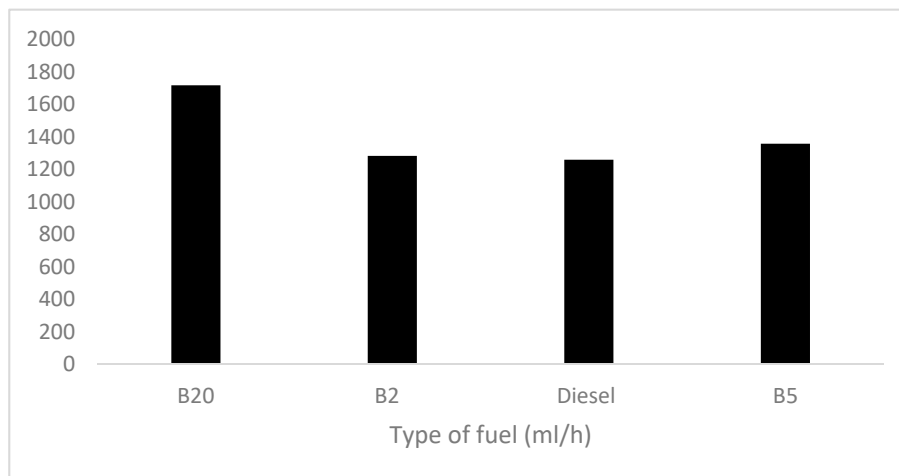


Figure 8. Average fuel consumption.

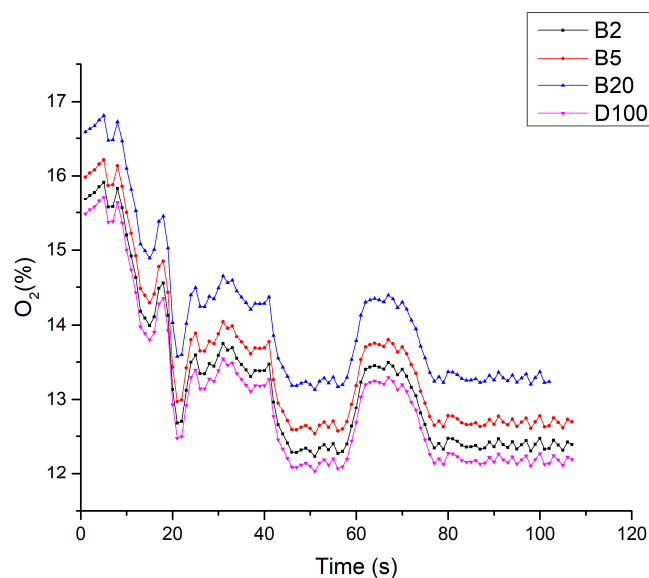


Figure 9. Oxygen emission of the fuels.

Figure 10 shows the behavior of the CO exhaust gases emitted by the CI-Engine when the different mixtures are burned. The amount of emissions is increased when the engine load and rpm increases, but they decreased when the biodiesel concentration of the mixture is increased, similar to the results reported by Di et al. [45]. At low speeds there is a low temperature of the combustion gases inside the combustion chamber, this avoids the CO becoming CO₂ [46]. In general, a reduction of CO was obtained by the substitution of diesel to biodiesel, with an emission of 156 ppm by the diesel, 126 ppm by B20 mixture, 139 ppm by B5 mixture, and 146 ppm by B2 mixture. Concerning diesel, an emissions

reduction was obtained on average of 18%, 10%, and 6%, respectively. In general, the biodiesel has approx. 10% of the oxygen on a mass basis and has a lower carbon content of carbon than diesel, thus the ignition delay can be shortened, and the combustion efficiency increases with the oxygen in the fuel favoring the reduction of CO emissions [47].

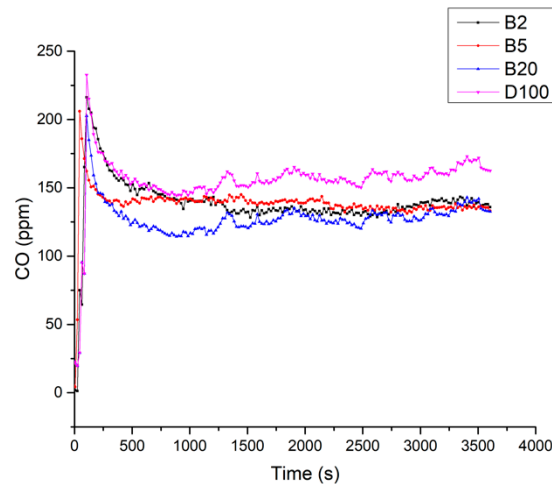


Figure 10. CO emissions of the fuels on average.

Figure 11 displays the average of SO_2 emissions from fuels. There was a difference between D100 and B20 with a 2.6% reduction of SO_2 [47]. This is because the CIE is working with 850 rpm, several authors agree that being a biofuel of vegetal origin there is no sulfur in the combustion of biodiesel from soybean oil, contributing to the decrease of sulfur dioxide in the CIE's emissions, meanwhile for diesel, values were up to 20% higher than biodiesel, and the results agree with those reported in [47–49]. When the biodiesel concentration of the mixture percentage increases the oxygen, the content increases to bring about a decrease in combustion fumes, this explains why the oxygen content in the fuel contributes to the complete oxidation of fuel [49]. The variability of the biodiesel properties can affect the CIE's in terms of gas emissions such as nitrogen oxide and carbon oxide. The nitric oxide (NO) is produced in greater amounts and predominates in the NO_x production inside the combustion chamber when the combustion is performed with small portions of nitrogen dioxide (NO_2). Some authors measure the NO_x , which is the summary of NO and NO_2 , by a chemiluminescence analyzer [50]. The measurements of the NO of the exhaust manifold using commercially available equipment for measurement of combustion gases of CIE's is considered a good approximation [51]. The experimental studies for measurement have shown that the NO_x emissions vary according to the biodiesel composition; the degree of saturation of biodiesel, the longer and more saturated chain esters increase the cetane number (CN) of biodiesel and tend to decrease the NO_x [52]. It is important to mention that the authors of this work did not focus on analyzing the NO_x gas, however, during the tests the variation of this gas is observed, in [53], the authors publish an analysis of the behavior of the NO_x , also the portions of optimal mixtures to mitigate the high emissions of this harmful gas, also in [52,54–58], the authors present some solutions to this problem. The biodiesel chemical instauration, the biodiesel oxidative degradation, the relative stoichiometry the calorific value, the characteristics of the fuel spray, the type of biodiesel (methyl or ethyl ester), the oxygen availability, and the levels of aromatic compounds can be factors that influence the NO_x emissions, because of its direct effects on flame temperature inside the combustion chamber of the engine [59].

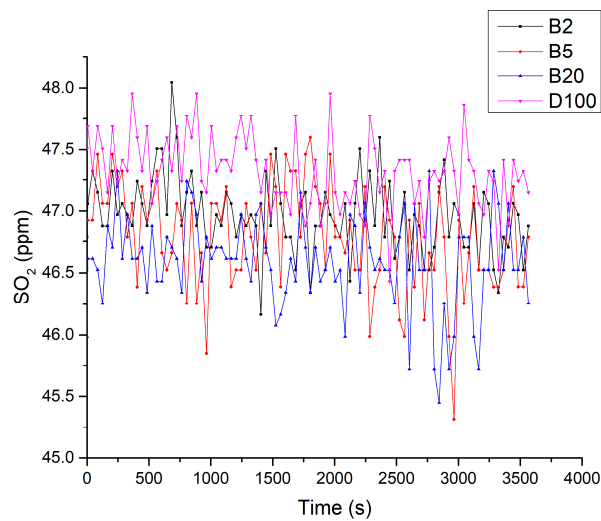


Figure 11. Average SO_2 emissions by fuels.

Figure 12 illustrates the results of NO gas emissions not registered in the exhaust manifold on the engine working with all the mixtures. In general, the behavior does not have a significant change in the CO emissions of the engine, although the engine when working with B20 has obtained NO emissions on average of 72 ppm and only 3% less NO emissions than D100.

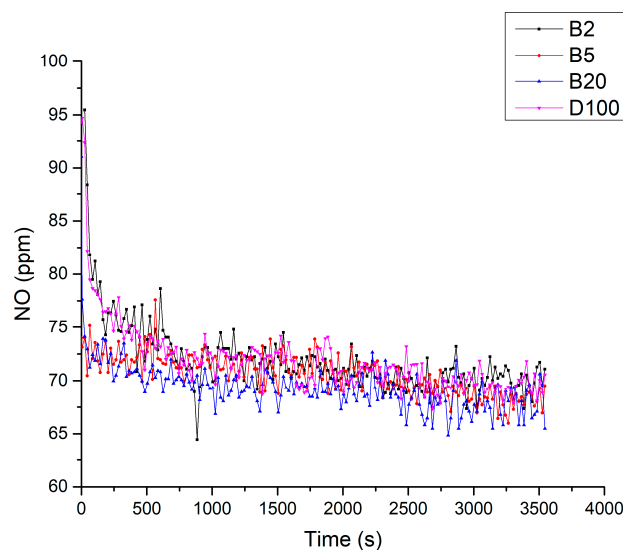


Figure 12. Average of NO emissions of the fuels.

4. Conclusions

The VIMEP developed is an innovative and flexible virtual instrument based in the programming platform LabVIEW 2015, which can be adapted to characterize internal combustion engines as diesel using biofuel mixtures. The programming of VI that was used is shown in a general way. The VI is trustworthy and has a low price, with which the rpm, fuel consumption, temperatures and CO, O_2 , NO, and SO_2 emissions parameters can be registered. When the biodiesel concentration in the mixtures increase, the calorific power decreases 2.8% for B20, 1.3% for B5, and 0% for B2. For viscosity, there is an increase of 4% for B20, 2% for B5, and B2 has the same value as D100.

The B20 mixture registered a lower emission of CO than the D100 emission. This result was obtained by operating the engine at 850 rpm as regime because the engine is not submitted to an electric charge and does not demand power and this decrease is due to biodiesel being a more oxygenated

fuel. The levels of NO emitted when the B20 is combusted were slightly lower or like NO emitted by burning 100% diesel with just 3% of NO in ppm. The results obtained for SO₂ gas are very similar in the reduction percentages with just 2.6% of SO₂ decrease for B20 compared to D100, this was mainly due to the biodiesel being obtained from a new soybean oil, a feedstock that does not contain sulfur and has more oxygen availability to carry out the combustion process. The emission values obtained are below the limits allowed by the Official Mexican Standard NOM-044-SEMARNAT-2017. This result is expected as the engine was mounted on a test bench. The engine was operating in conditions of low and constant speed without power demand.

The infrared spectroscopy is an accessible technique that has shown an appropriate methodology to quantify the percentages of biodiesel mixture of cooking oil in a concentration range of 5–70%, taking as standard the increase of the carbonyl group attenuation as the biodiesel mixture concentrations increase. It can be deduced that this concentration range fulfills the law of the Beer–Lambert.

Author Contributions: Substantial contributions to the conception of the results was carried out by A.P. and D.M.; Methodology and analysis was conceptualized out by C.C.; The validation and formal analysis of the results was carried out by M.C. and C.G.; The final approval of the version was evaluated by G.M. and B.V. All authors read and approved the final manuscript.

Funding: This research received no external funding

Acknowledgments: The authors thank the National Council of Science and Technology CONACYT Mexico, Faculty of Engineering and Technology Sciences, Autonomous University of Baja California, and the Institute of Engineering of the Autonomous University of Baja California for their support in the development of this work.

Conflicts of Interest: The authors declare no conflict of interest.

References

- Asif, M.; Muneer, T. Energy supply, its demand and security issues for developed and emerging economies. *Renew. Sustain. Energy Rev.* **2007**, *11*, 1388–1413. [[CrossRef](#)]
- Dincer, I. Environmental impacts of energy. *Energy Policy* **1999**, *27*, 845–854. [[CrossRef](#)]
- Kalam, M.A.; Hassan, M.; Jayed, M.; Liaquat, A. Emission and performance characteristics of an indirect ignition diesel engine fuelled with waste cooking oil. *Energy* **2011**, *36*, 397–402. [[CrossRef](#)]
- BP. *BP Statistical Review of World Energy June 2017*; BP: London, UK, 2017.
- International Renewable Energy Agency (IRENA). *Global Energy Transformation: A Roadmap to 2050*; IRENA: Abu Dhabi, UAE, 2018. [[CrossRef](#)]
- Lee, H.V.; Juan, J.C.; Taufiq-Yap, Y.H.; Kong, P.S.; Rahman, N.A. Advancement in heterogeneous base catalyzed technology: An efficient production of biodiesel fuels. *J. Renew. Sustain. Energy* **2015**, *7*, 032701. [[CrossRef](#)]
- Ali, O.M.; Mamat, R.; Abdullah, N.R.; Abdullah, A.A. Analysis of blended fuel properties and engine performance with palm biodiesel–diesel blended fuel. *Renew. Energy* **2016**, *86*, 59–67. [[CrossRef](#)]
- Ma, F.; A Hanna, M. Biodiesel production: A review. *Bioresour. Technol.* **1999**, *70*, 1–15. [[CrossRef](#)]
- Espinosa, E.A.M.; Piloto-Rodríguez, R.; Goyos-Pérez, L.; Sierens, R.; Verhelst, S. Emulsification of animal fats and vegetable oils for their use as a diesel engine fuel: An overview. *Renew. Sustain. Energy Rev.* **2015**, *47*, 623–633. [[CrossRef](#)]
- Igbum, O.G.; Eloka-Eboka, A.C.; Ubwa, S.T.; Inambao, F.L. Evaluation of environmental impact and gaseous emissions of biodiesel fuels and blends of selected feed-stocks. *Int. J. Glob. Warm.* **2014**, *6*, 99. [[CrossRef](#)]
- Dorado, M.P.; Ballesteros, E.; Arnal, J.M.; Gómez, J.; López, F.J. Exhaust emissions from a Diesel engine fueled with transesterified waste olive oil. *Fuel* **2003**, *82*, 1311–1315. [[CrossRef](#)]
- Atadashi, I.; Aroua, M.K.; Aziz, A.A. High quality biodiesel and its diesel engine application: A review. *Renew. Sustain. Energy Rev.* **2010**, *14*, 1999–2008. [[CrossRef](#)]
- Rakopoulos, C.D.; Antonopoulos, K.; Rakopoulos, D.; Hountalas, D.; Giakoumis, E.G. Comparative performance and emissions study of a direct injection Diesel engine using blends of Diesel fuel with vegetable oils or bio-diesels of various origins. *Energy Convers. Manag.* **2006**, *47*, 3272–3287. [[CrossRef](#)]
- Graboski, M.S.; McCormick, R.L. Combustion of fat and vegetable oil derived fuels in diesel engines. *Prog. Energy Combust. Sci.* **1998**, *24*, 125–164. [[CrossRef](#)]

15. Claxton, L. The history, genotoxicity, and carcinogenicity of carbon-based fuels and their emissions. Part 3: Diesel and gasoline. *Mutat. Res. Mutat. Res.* **2015**, *763*, 30–85. [CrossRef] [PubMed]
16. Borillo, G.C.; Tadano, Y.S.; Godoi, A.F.L.; Pauliquevis, T.; Sarmiento, H.; Rempel, D.; Yamamoto, C.I.; Marchi, M.R.; Potgieter-Vermaak, S.; Godoi, R. Polycyclic Aromatic Hydrocarbons (PAHs) and nitrated analogs associated to particulate matter emission from a Euro V-SCR engine fuelled with diesel/biodiesel blends. *Sci. Total. Environ.* **2018**, *644*, 675–682. [CrossRef]
17. Testo 340—Flue gas analyzer for industry | Metal and steel | Emissions | Industry | Target groups. Available online: <https://www.testo.com/en-US/testo-340/p/0632-3340> (accessed on 13 June 2019).
18. Gas Analyzer Enerac 700—Portable Combustion Analyzer. Available online: <http://www.enerac.com/gas-analyzer-enerac-700/> (accessed on 13 June 2019).
19. Bonilla, D.; Gil Samaniego, M.; Gil-Samaniego, M.; Campbell, H. Practical and low-cost monitoring tool for building energy management systems using virtual instrumentation. *Sustain. Cities Soc.* **2018**, *39*, 155–162. [CrossRef]
20. Goldberg, H. What is virtual instrumentation? *IEEE Instrum. Meas. Mag.* **2000**, *3*, 10–13. [CrossRef]
21. Manigandan, S.; Gunasekar, P.; Devipriya, J.; Nithya, S. Emission and injection characteristics of corn biodiesel blends in diesel engine. *Fuel* **2019**, *235*, 723–735. [CrossRef]
22. Moore, K. *Testing Automotive Exhaust Emissions—Application Note*; National Instruments: Austin, TX, USA, 2013.
23. Pérez, A.; Ramos, R.; Montero, G.; Coronado, M.; García-González, C.; Pérez, R. Virtual Instrument for Emissions Measurement of Internal Combustion Engines. *J. Anal. Methods Chem.* **2016**, *2016*, 1–13. [CrossRef]
24. Frijters, P.; Baert, R. Oxygenated fuels for clean heavy-duty diesel engines. *Int. J. Veh. Des.* **2006**, *41*, 242. [CrossRef]
25. Sahoo, P.; Das, L.; Babu, M.; Arora, P.; Singh, V.; Kumar, N.; Varyani, T. Comparative evaluation of performance and emission characteristics of jatropha, karanja and polanga based biodiesel as fuel in a tractor engine. *Fuel* **2009**, *88*, 1698–1707. [CrossRef]
26. Chauhan, B.; Kumar, N.; Cho, H.M. A study on the performance and emission of a diesel engine fueled with Jatropha biodiesel oil and its blends. *Energy* **2012**, *37*, 616–622. [CrossRef]
27. Tesfa, B.; Gu, F.; Mishra, R.; Ball, A.D. Emission Characteristics of a CI Engine Running with a Range of Biodiesel Feedstocks. *Energies* **2014**, *7*, 334–350. [CrossRef]
28. Hansen, A.C.; Gratton, M.R.; Yuan, W. Diesel Engine Performance and NOX Emissions From Oxygenated Biofuels and Blends with Diesel Fuel. *Trans. ASABE* **2006**, *49*, 589–595. [CrossRef]
29. Canakci, M. NOx emissions of biodiesel as an alternative diesel fuel. *Int. J. Veh. Des.* **2009**, *50*, 213. [CrossRef]
30. Kim, H.; Choi, B. The effect of biodiesel and bioethanol blended diesel fuel on nanoparticles and exhaust emissions from CRDI diesel engine. *Renew. Energy* **2010**, *35*, 157–163. [CrossRef]
31. Xue, J.; Grift, T.E.; Hansen, A.C. Effect of biodiesel on engine performances and emissions. *Renew. Sustain. Energy Rev.* **2011**, *15*, 1098–1116. [CrossRef]
32. Cardoso, C.C.; Mendes, B.M.; Pasa, V.M.D. Production and characterization of cold-flow quality biofuel from soybean oil using different alky and benzyl alcohols. *J. Environ. Chem. Eng.* **2018**, *6*, 2241–2247. [CrossRef]
33. Martínez, A.; Mijangos, G.E.; Romero-Ibarra, I.; Hernández-Altamirano, R.; Mena-Cervantes, V.Y. In-situ transesterification of Jatropha curcas L. seeds using homogeneous and heterogeneous basic catalysts. *Fuel* **2019**, *235*, 277–287. [CrossRef]
34. Reyero, I.; Arzamendi, M.C.; Zabala, S.; Gandía, L.M. Kinetics of the NaOH-catalyzed transesterification of sunflower oil with ethanol to produce biodiesel. *Fuel Process. Technol.* **2015**, *129*, 147–155. [CrossRef]
35. Versión, N. PEMEX DIESEL Hoja de Datos de Seguridad SECCIÓN I. DATOS GENERALES. n.d. Available online: <https://www.pemex.com/negocio/gasolineras/nuestros-productos/Documents/HDS-Pemex%20Diesel.pdf> (accessed on 18 February 2019).
36. Pullen, J.; Saeed, K. Factors affecting biodiesel engine performance and exhaust emissions—Part I: Review. *Energy* **2014**, *72*, 1–16. [CrossRef]
37. Benavides, A.; Benjumea, P.; Pashova, V. El biodiesel de aceite de higuera como combustible alternativo para motores diesel. *Dyna* **2007**, *74*, 141–150.
38. Mattarelli, E.; Rinaldini, C.A.; Savioli, T. Combustion Analysis of a Diesel Engine Running on Different Biodiesel Blends. *Energies* **2015**, *8*, 3047–3057. [CrossRef]

39. Heise, H.M.; Fritzsche, J.; Tkatsch, H.; Waag, F.; Karch, K.; Henze, K.; Delbeck, S.; Budde, J. Recent advances in mid- and near-infrared spectroscopy with applications for research and teaching, focusing on petrochemistry and biotechnology relevant products. *Eur. J. Phys.* **2013**, *34*, S139–S159. [CrossRef]
40. Soares, I.P.; Rezende, T.F.; Pereira, R.D.C.C.; Dos Santos, C.G.; Fortes, I.C.P. Determination of biodiesel adulteration with raw vegetable oil from ATR-FTIR data using chemometric tools. *J. Braz. Chem. Soc.* **2011**, *22*, 1229–1235. [CrossRef]
41. Aliske, M.A.; Zagonel, G.F.; Costa, B.J.; Veiga, W.; Saul, C. Measurement of biodiesel concentration in a diesel oil mixture. *Fuel* **2007**, *86*, 1461–1464. [CrossRef]
42. Aryee, A.N.A.; van de Voort, F.R.; Simpson, B.K. *Process Biochemistry*; Elsevier Science: Amsterdam, The Netherlands, 2009; Volume 44.
43. Buyukkaya, E. Effects of biodiesel on a DI diesel engine performance, emission and combustion characteristics. *Fuel* **2010**, *89*, 3099–3105. [CrossRef]
44. Knothe, G.; Krahl, J.; Van Gerpen, J.H. *The Biodiesel Handbook*; AOCS Press: Urbana, IL, USA, 2010.
45. Di, Y.; Cheung, C.S.; Huang, Z. Experimental investigation on regulated and unregulated emissions of a diesel engine fueled with ultra-low sulfur diesel fuel blended with biodiesel from waste cooking oil. *Sci. Total. Environ.* **2009**, *407*, 835–846. [CrossRef] [PubMed]
46. Lin, C.-Y.; Lin, H.-A. Diesel engine performance and emission characteristics of biodiesel produced by the peroxidation process. *Fuel* **2006**, *85*, 298–305. [CrossRef]
47. Lin, Y.-F.; Wu, Y.-P.G.; Chang, C.-T. Combustion characteristics of waste-oil produced biodiesel/diesel fuel blends. *Fuel* **2007**, *86*, 1772–1780. [CrossRef]
48. Canakci, M. Combustion characteristics of a turbocharged DI compression ignition engine fueled with petroleum diesel fuels and biodiesel. *Bioresour. Technol.* **2007**, *98*, 1167–1175. [CrossRef]
49. Lapuerta, M.; Fernández, J.R.; Agudelo, J.R. Diesel particulate emissions from used cooking oil biodiesel. *Bioresour. Technol.* **2008**, *99*, 731–740. [CrossRef]
50. Heywood, J.B. *Internal Combustion Engine Fundamentals*; McGraw-Hill Inc: New York, NY, USA, 1998.
51. Norris, J. *EMStec-Unclassified an In-Service Emissions Test for Spark Ignition (SI) Petrol Engines-PPAD 9/107/09*; Phase 2b Report Identification of options for alternative test procedures; A report produced for DfT; 2002. Available online: https://uk-air.defra.gov.uk/assets/documents/reports/cat15/0408171322_SI_Phase2aReport.pdf (accessed on 22 September 2019).
52. Graboski, M.S.; McCormick, R.L.; Alleman, T.L.; Herring, A.M. *The Effect of Biodiesel Composition on Engine Emissions from a DDC Series 60 Diesel Engine: Final Report*. Report 2 in a Series of 6. 2003. 2003. Available online: <https://pdfs.semanticscholar.org/7bd3/35e0bd81f41601152303fd4093b697f24d59.pdf> (accessed on 14 April 2019).
53. Varatharajan, K.; Cheralathan, M.; Velraj, R. Mitigation of NOx emissions from a jatropha biodiesel fuelled DI diesel engine using antioxidant additives. *Fuel* **2011**, *90*, 2721–2725. [CrossRef]
54. Hess, M.A.; Haas, M.J.; Foglia, T.A.; Marmer, W.N. Effect of Antioxidant Addition on NOx Emissions from Biodiesel. *Energy Fuels* **2005**, *19*, 1749–1754. [CrossRef]
55. McCormick, R.L.; Alvarez, J.R.; Graboski, M.S. *NOx Solutions for Biodiesel: Final Report*; Report 6 in a Series of 6; Office of Scientific and Technical Information (OSTI): Washington, DC, USA, 2003; p. 6.
56. Varatharajan, K.; Cheralathan, M. Effect of aromatic amine antioxidants on NOx emissions from a soybean biodiesel powered DI diesel engine. *Fuel Process. Technol.* **2013**, *106*, 526–532. [CrossRef]
57. Ileri, E.; Kocar, G. Experimental investigation of the effect of antioxidant additives on NOx emissions of a diesel engine using biodiesel. *Fuel* **2014**, *125*, 44–49. [CrossRef]
58. Palash, S.; Kalam, M.A.; Hassan, M.; Masum, B.; Fattah, I.M.R.; Mofijur, M. Impacts of biodiesel combustion on NOx emissions and their reduction approaches. *Renew. Sustain. Energy Rev.* **2013**, *23*, 473–490. [CrossRef]
59. Sun, J.; Caton, J.A.; Jacobs, T.J. Oxides of nitrogen emissions from biodiesel-fuelled diesel engines. *Prog. Energy Combust. Sci.* **2010**, *36*, 677–695. [CrossRef]

